Non-Fermi-liquid behavior in $CaCu_3Ru_4O_{12}$

A. Krimmel,* A. Günther, W. Kraetschmer, H. Dekinger, N. Büttgen, and A. Loidl
Experimental Physics V, Center for Electronic Correlations and Magnetism, University of Augsburg, 86135 Augsburg, Germany

S. G. Ebbinghaus
Institut für Chemie, Martin-Luther-Universität Halle-Wittenberg, 06120 Halle (Saale), Germany

E.-W. Scheidt and W. Scherer
CPM, Institute of Physics, University of Augsburg, 86135 Augsburg, Germany

(Received 24 July 2008; revised manuscript received 2 October 2008; published 29 October 2008)

We present bulk magnetic susceptibility, specific heat, transport, NMR, and NQR results of the perovskite compound $CaCu_3Ru_4O_{12}$. The data consistently describe a metallic state with a moderately enhanced Sommerfeld coefficient of $\gamma=92$ mJ/mol K^2 and a spin-fluctuation temperature of about 180 K. The heat capacity below 2 K shows a logarithmic increase providing evidence for non-Fermi-liquid (NFL) behavior in $CaCu_3Ru_4O_{12}$. Further signatures of NFL properties are found in NQR measurements revealing deviations from a Korringa behavior of the spin-lattice relaxation rate. The results are discussed with respect to heavy-fermion and NFL properties in other transition-metal compounds and traditional *f*-electron systems.

DOI: 10.1103/PhysRevB.78.165126 PACS number(s): 65.40.Ba, 71.27.+a, 71.10.Hf

I. INTRODUCTION

Transition-metal compounds crystallizing in the perovskite or its derivative structures are the focus of current solid-state research since they exhibit the most diverse types of physical properties including such spectacular phenomena such as high-temperature superconductivity, colossal magnetoresistance effects, strong magnetoelectric coupling, and high dielectric constants to mention just a few. In the case where three fourths of the *A*-site cations of the parent perovskite ABO_3 are substituted by Jahn-Teller active ions, the unit cell doubles in all three directions and a new crystallographic *C* site appears due to a collective rotation of the BO_6 octahedra around the crystallographic ⟨111⟩ direction. These compounds are then described by the stoichiometry $AC_3B_4O_{12}$. The *C*-site cations are in a square planar oxygen coordination analogous to the Cu-O planes of the high-T_c cuprate superconductors and the *A*-site ions are in an icosahedral oxygen environment. In the structure of $AC_3B_4O_{12}$ a large variety of cations of sufficient size can fill the *A* or *B* site largely independent of their oxidation state, whereas the *C* site is usually occupied by Cu^{2+} or Mn^{3+} ions. Two prominent examples are $CaCu_3Ti_4O_{12}$ and $CaCu_3Mn_4O_{12}$. The former compound has been extensively studied with respect to colossal dielectric properties,[1,2] whereas the latter is a ferromagnet with a record ordering temperature of $T_C=360$ K and large magnetoresistance.[3,4]

Recently, $CaCu_3Ru_4O_{12}$ has been described as a *d*-electron-based heavy-fermion compound[5] with a Kondo temperature of about 200 K and a moderately enhanced Sommerfeld coefficient of $\gamma=85$ mJ/mol K^2. Traditional *f*-electron-based heavy-fermion states are formed via hybridization between two different electronic subsystems, namely, localized *f* electrons and band states of conduction electrons. This results in a highly enhanced density of states at the Fermi level (Abrikosov-Suhl resonance) and a concomitant quasiparticle renormalization described by an enhanced effective electronic mass $m^*/m_e=1\times10^2-10^3$. However, it has been demonstrated that heavy-fermion behavior should also occur in transition-metal oxides upon approaching a metal-insulator transition.[6] Recent x-ray spectroscopic measurements revealed here that $CaCu_3Ru_4O_{12}$ is a direct analog-to-conventional *f*-electron heavy fermions based on localized magnetic moments of the Cu^{2+} ions and itinerant *d* electrons originating from strong Ru-O hybridization.[7] Localized and itinerant electrons are supposed to be coupled antiferromagnetically by the Kondo mechanism.[7]

In this paper, we report on heat capacity, bulk magnetic, NMR or nuclear quadrupole resonance (NQR), and transport properties of $CaCu_3Ru_4O_{12}$ to gain deeper insight into its unusual ground state. Most importantly, the specific-heat data and the NQR spin-lattice relaxation rate at low temperatures provide strong evidence for non-Fermi-liquid (NFL) behavior.

II. EXPERIMENTAL DETAILS

Polycrystalline samples of $CaCu_3Ru_4O_{12}$ were synthesized by a solid-state reaction. Stoichiometric amounts of high-purity (4N) $CaCO_3$, CuO, and RuO_2 were dried, mixed, and calcined in air at 1050 °C for 20 h in alumina crucibles. To assure complete chemical reaction and to achieve single-phase material with good homogeneity, the sintering process at 1050 °C was repeated several times with subsequent regrinding, pressing, and firing. The polycrystalline samples were characterized by x-ray powder diffraction employing Cu-$K_{\alpha1}$ radiation. The data were analyzed by standard Rietveld refinement using the FULLPROF program suite.[8] Additionally, high-resolution single-crystal x-ray diffraction on $CaCu_3Ru_4O_{12}$ was performed at low temperatures, $T=7$ K. These single crystals were prepared in CuO flux. Bragg reflections were collected on a MAR345 imaging plate detector system with a rotating anode generator using Mo-K_α radiation of wavelength $\lambda=0.710\,73$ Å. Magnetic measurements were performed in a commercial superconducting

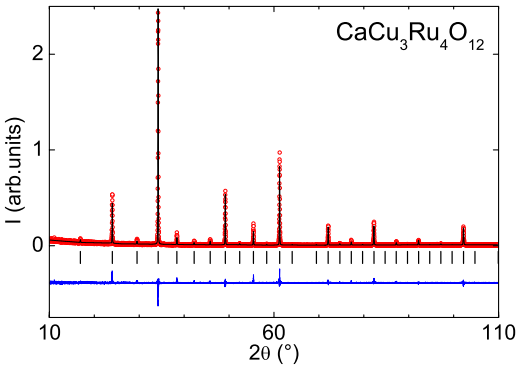

FIG. 1. (Color online) Room-temperature powder x-ray diffraction pattern of $CaCu_3Ru_4O_{12}$. Measured (open red circles) and calculated (black line) intensities, as well as their difference (blue line at the bottom) and corresponding Bragg-peak positions (vertical bars) are shown.

quantum interference device (SQUID) magnetometer for temperatures of $1.8 \leq T \leq 400$ K and fields up to 5 T. Four-point resistivity measurements were performed on pressed and sintered ceramics for $1.5 \leq T \leq 280$ K. The heat capacity was investigated in a physical properties measurement system (PPMS) in the temperature range $2 \leq T \leq 300$ K in zero field and in an external field of 7 T. Specific-heat measurements were extended down to 60 mK in a ^{3}He/^{4}He dilution cryostat using a relaxation method.[9] NMR and NQR measurements were performed using a phase-coherent pulse spectrometer and spin-echo techniques. NMR spectra were collected by the field-sweep method within the temperature range $1.6 \leq T \leq 275$ K at the constant irradiation frequencies of $\omega_0/2\pi = 50.25$ and 17 MHz in the case of the ^{63,65}Cu and ^{99}Ru isotopes, respectively. NQR measurements of spectra and spin-lattice relaxation rates $1/T_1$ were additionally conducted down to 190 mK in a top-loading ^{3}He/^{4}He dilution cryostat with the sample inside the mixing chamber. The spin-lattice relaxation rates $1/T_1$ were obtained from NQR experiments in zero external magnetic field employing an inversion-recovery pulse sequence, where $\tau = 4$ μs was the length of the inversion pulse.

III. SAMPLE CHARACTERIZATION

A. X-ray diffraction

X-ray powder diffraction at room temperature revealed single-phase material without any indications of spurious phases. Figure 1 shows the corresponding diffraction pattern of $CaCu_3Ru_4O_{12}$. The crystal structure of $CaCu_3Ru_4O_{12}$ can be considered as a $2 \times 2 \times 2$ superstructure of the parent perovskite structure of ABO_3. It is described by cubic symmetry with space group $Im\bar{3}$ and atomic positions of Ca at (0,0,0), Cu at $(\frac{1}{2},0,0)$, Ru at $(\frac{1}{4},\frac{1}{4},\frac{1}{4})$, and O at $(x,y,0)$. Refined structural parameters are thus the lattice constant $a = 7.4082(1)$ Å and the oxygen positional parameters $x = 0.1782(12)$ and $y = 0.3053(12)$. These values comply with those reported in the literature[10,11] and result in a good agreement between observed and calculated intensities, as reflected in a standard deviation of $\chi^2 = 2.09$ and a reliability factor of $R_{\mathrm{Bragg}} = 6.08\%$—illustrated in Fig. 1.

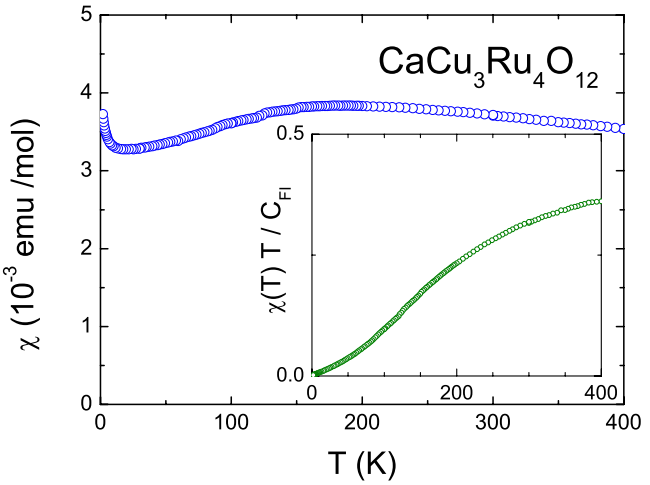

FIG. 2. (Color online) Temperature-dependent magnetic susceptibility of polycrystalline $CaCu_3Ru_4O_{12}$ in an external field of $\mu_0 H = 1$ T. The inset shows $\chi(T)T/C_{\mathrm{FI}}$ versus T to determine the spin-fluctuation temperature T_{SF}, as described in text.

Additional high-resolution single-crystal x-ray diffraction of $CaCu_3Ru_4O_{12}$ at $T = 7$ K was performed using a black prism with the dimensions $0.05 \times 0.05 \times 0.08$ mm^3. The data set was corrected for beam inhomogeneity and absorption effects, and symmetry equivalent and multiple measured reflections were averaged[12] yielding 542 independent reflections. The symmetry is preserved down to 7 K. Structural refinements based on F^2 were performed with SHELXL-97.[13] The refinement of 15 parameters against 525 observed reflections [for $F > 4\sigma(F)$] converged to $R_1 = 0.0326$, $wR_2 = 0.108$, GOF=1.29, and a featureless residual electron density of $2.21/-2.54$ e/Å^3 ($0.38/-0.49$ e/Å^3 for $2\theta < 50°$). Refining the fractional atomic occupancies resulted in the nominal stoichiometry of our parent compound. The lattice constant is $a = 7.4098(2)$ Å and the oxygen position $(x,y,0)$ was determined to be $x = 0.174\,75(18)$ and $y = 0.307\,43(18)$, which is in good agreement with the powder-diffraction data at ambient temperature (see above). The high-resolution data at low temperature clearly reveal the presence of merohedral twinning domains with a twin ratio of 90.2(6)/9.8(6) and a twin law of (010 001 100), which are in contrast to previous findings in the literature.[14]

B. Magnetic susceptibility

Figure 2 shows the magnetic susceptibility of polycrystalline $CaCu_3Ru_4O_{12}$. In agreement with previous measurements,[5] only a weak temperature dependence of an enhanced Pauli susceptibility is observed with a broad maximum around 180 K. With reference to an analogous behavior in $CeSn_3$ this maximum was identified with the Kondo temperature.[5] A high Kondo temperature indicates a strong hybridization that enables charge fluctuations, and thus, puts these systems into the class of mixed-valent compounds. Usually, $CeSn_3$ is considered as a prototypical representative of these materials. Below room temperature, the susceptibility of mixed-valent compounds can vary considerably de-

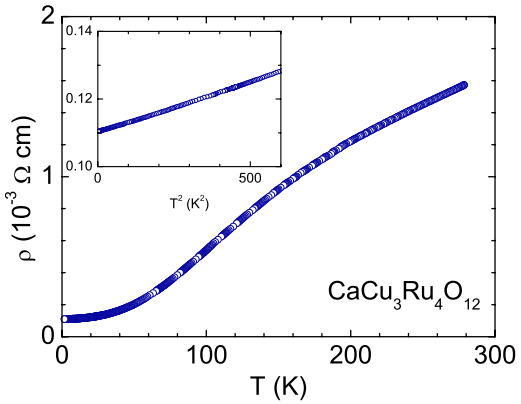

FIG. 3. (Color online) Temperature-dependent resistivity of polycrystalline $CaCu_3Ru_4O_{12}$. The inset shows the low-temperature part of the polycrystalline sample on a T^2 scale.

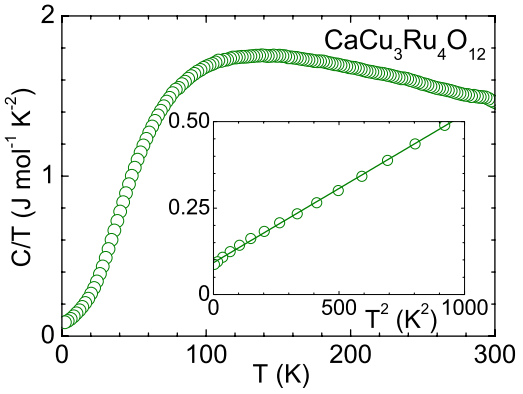

FIG. 4. (Color online) Specific heat $C/T(T)$ of polycrystalline $CaCu_3Ru_4O_{12}$ (main frame) and a representation C/T versus T^2 (inset). A conventional metallic Fermi-liquid behavior according to $C(T)=\gamma T+\beta T^3$ (solid line of the inset) is observed for $T>2$ K.

pending on the characteristic spin-fluctuation temperature T_{SF}. For example, $CeSn_3$ reveals a high-temperature Curie-Weiss law above 200 K, followed by a broad maximum around 150 K, and turns into an enhanced Pauli susceptibility below 40 K.[15] On the other hand, mixed-valent $CeRu_2$ shows an almost temperature-independent Pauli susceptibility at least up to 400 K.[16] In general, a Curie behavior due to localized paramagnetic moments is expected well above T_{SF}, whereas an enhanced Pauli susceptibility is expected well below T_{SF}. A convenient way to visualize this variation in the magnetic properties is a plot of $\chi(T)T/C_{FI}$ versus T with $C_{FI}=1.21$ emu K/mol being the calculated free-ion Curie constant. At high temperature, a Curie law leads to a saturated value of $\chi(T)T/C_{FI}\approx 1$ and a linear decrease at low temperature corresponding to a constant Pauli susceptibility. The temperature where $\chi(T)T/C_{FI}\approx 0.5$ then can be identified with T_{SF}. A nice compilation of the susceptibility data of Ce- and Yb-based mixed-valent compounds was published by Kishimoto *et al.*[17] In traditional correlated f-electron systems, the Wilson ratio $R_W=\pi^2 k_B^2\chi(0)/g^2J(J+1)\mu_B^2\gamma$ adopts a value[18] of $1+2/2J$. This allows an estimation of the residual susceptibility $\chi(0)$ that is subtracted from the experimentally determined susceptibility. The corresponding plot of $\chi(T)T/C_{FI}$ versus T of $CaCu_3Ru_4O_{12}$ is shown in the inset of Fig. 2. Obviously, $\chi(T)T/C_{FI}$ does not reach 0.5 within the investigated temperature range. A linear extrapolation of the data toward higher temperatures would result in a high spin-fluctuation temperature of about $T_{SF}\approx 850$ K. This behavior is rather similar[17] to that observed in $CeRu_2$. The magnetic susceptibility in $CaCu_3Ru_4O_{12}$ is also consistent with the temperature-dependent NMR Knight shift which similarly reveals a broad maximum around 180 K (not shown). In contrast to the susceptibility data shown in Fig. 2, a Curie-type upturn of the Knight shift is not observed at low temperatures, confirming its origin to be due to a small amount of local magnetic defects.

C. Electrical resistivity

Figure 3 shows the electrical resistivity of polycrystalline $CaCu_3Ru_4O_{12}$ for $1.5\leq T\leq 280$ K. Metallic conductivity $(d\rho/dT>0)$ is observed in the entire temperature range with a quadratic temperature dependence $\rho(T)=\rho_0+AT^2$ for $T<25$ K (characteristic of a Fermi liquid), as illustrated in the inset of Fig. 3. The residual resistivity is $\rho_0(T=1.5\text{ K})=0.110(3)$ mΩ cm and the coefficient is $A=2.95(3)1\times 10^{-5}$ mΩ cm/K^2. No significant difference could be observed for measurements in zero field and in an external field of 14 T. In the following, we focus on heat capacity, NMR, and NQR experiments of polycrystalline samples to study the low-temperature properties of $CaCu_3Ru_4O_{12}$.

D. Specific heat ($T\geq 2$ K)

The heat capacity $C/T(T)$ of $CaCu_3Ru_4O_{12}$, as shown in Fig. 4, exhibits a conventional behavior of metallic Fermi liquids for $T>2$ K according to $C(T)=\gamma T+\beta T^3$. The phononic contribution results in a Debye temperature of $\Theta_D=451$ K and the electronic part is described by a Sommerfeld coefficient of $\gamma=92\pm 2$ mJ/Mol K^2 or, normalized per Cu spin, 30.7 ± 2 mJ/Cu K^2. The moderately enhanced value of the Sommerfeld coefficient is a characteristic of a correlated metal, which is in agreement with previous reports.[5] It is also consistent with the values of the phenomenological parameters of the Kadowaki-Woods ratio $R_{KW}=A/\gamma^2=3.5\times 10^{-6}$ Ω cm mol^2 K^2/J^2 and the Wilson ratio $R_W=\pi^2 k_B^2\chi/3\mu_B^2\gamma=2.78$. A Kondo temperature may be estimated by $T_K=n\pi R/3\gamma$ with R being the gas constant and $n=3$ being the number of Cu ions per formula unit resulting in $T_K\approx 870$ K. The values of the Kondo temperature T_K, the spin-fluctuation temperature T_{SF}, and the Sommerfeld coefficient $\gamma=30.7$ mJ/Cu K^2 are mutually consistent and very close to those found for $CeRu_2$ (Ref. 17 and references therein).

E. NMR: Electric-field gradient

Figure 5 shows NMR and NQR spectra of the copper isotopes ^{63}Cu and ^{65}Cu (both carrying a nuclear spin of $I=3/2$) in $CaCu_3Ru_4O_{12}$. The upper frame displays the NMR spectrum of the central transitions $(-1/2\leftrightarrow+1/2)$ of ^{63}Cu and ^{65}Cu, which are split due to the electric-quadrupole in-

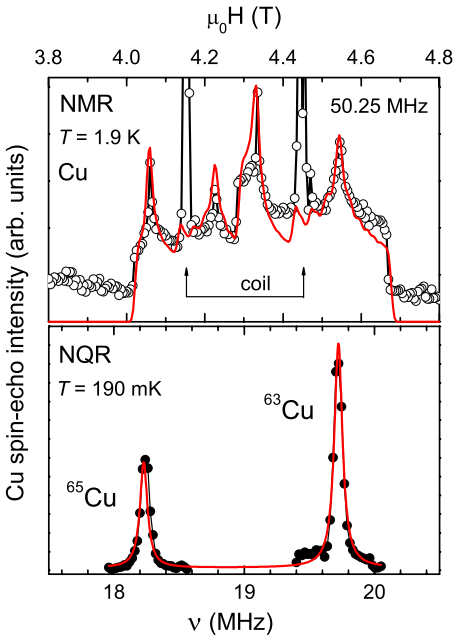

FIG. 5. (Color online) NMR and NQR spectra of polycrystalline $CaCu_3Ru_4O_{12}$. Upper frame: NMR spectrum of the $-1/2 \leftrightarrow 1/2$ transitions of the copper isotopes at $\omega = 50.25$ MHz and $T = 1.9$ K. The red solid line indicates the spectrum simulation of the quadrupolar perturbed Zeeman splitting (see text). The arrows denote the contributions due to the copper wire of the resonance coil. Lower frame: NQR spectra of the $\pm 1/2 \leftrightarrow \pm 3/2$ transitions of ^{65}Cu and ^{63}Cu at 190 mK. The red solid line is a fit with two Lorentzian lines (see text).

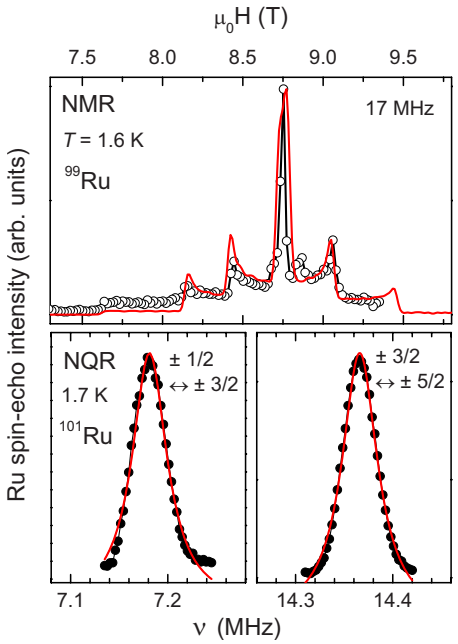

FIG. 6. (Color online) NMR and NQR spectra of polycrystalline $CaCu_3Ru_4O_{12}$. Upper frame: NMR spectrum of ^{99}Ru at $\omega = 17$ MHz and $T = 1.6$ K. The red solid line indicates the spectrum simulation of the quadrupolar perturbed Zeeman splitting (see text). Lower frame: NQR spectra of ^{101}Ru at 1.7 K. The red solid lines are fits with Lorentzian lines.

teraction between the nuclear quadrupole moments ($Q = -22 \times 10^{-30}$ m^2 for ^{63}Cu and $Q = -20.4 \times 10^{-30}$ m^2 for ^{65}Cu, respectively) and the local electric-field gradient which stems from the noncubic ionic coordination of the Cu site.[19] The solid line is a simulation of the NMR spectrum of the central transitions taking into account the quadrupole interaction up to second-order perturbation theory. Our parameters of the simulation agree with the results obtained in Ref. 19. The lower frame of Fig. 5 shows the NQR spectra of the $\pm 1/2 \leftrightarrow \pm 3/2$ transitions for ^{63}Cu and ^{65}Cu. The solid line is a fit with two Lorentzian lines considering the ratios of natural abundances (^{63}Cu/^{65}Cu = 2.24) and quadrupole moments ($^{63}Q/^{65}Q = 1.08$). From this fit we obtain the nuclear quadrupole frequencies $\nu_{NQR} = 18.23$ and 19.72 MHz for ^{65}Cu and ^{63}Cu, respectively. These values allow one to determine precisely the electric-field gradient at the copper site as $V_{zz}(\mathrm{Cu}) = 0.73 \times 10^{22}$ V/m^2.

Figure 6 shows NMR and NQR spectra of the ruthenium isotopes ^{99}Ru and ^{101}Ru (both isotopes with $I = 5/2$) in $CaCu_3Ru_4O_{12}$. The NMR experiment in the upper frame exhibits the nuclear resonance of the isotope ^{99}Ru only. Due to the vastly different quadrupole moments of the ruthenium isotopes ($Q = 7.9 \times 10^{-30}$ m^2 for ^{99}Ru and $Q = 45.7 \times 10^{-30}$ m^2 for ^{101}Ru, respectively), the NMR spectrum of ^{101}Ru is expected to be much broader and could not be detected. The lower frame of Fig. 6 shows the $\pm 1/2 \leftrightarrow \pm 3/2$ and $\pm 3/2 \leftrightarrow \pm 5/2$ transitions of ^{101}Ru yielding the value of the electric-field gradient at the ruthenium site [$V_{zz}(\mathrm{Ru}) = 0.43 \times 10^{22}$ V/m^2].

IV. NON-FERMI-LIQUID PROPERTIES

The main purpose of this work is to determine the low-temperature properties of $CaCu_3Ru_4O_{12}$, to search for possible NFL phenomena, or to find lower boundaries for the signatures of Fermi-liquid behavior, e.g., such as a square temperature dependence of the electrical resistivity (Fig. 3) or a pure Korringa relaxation.[20] On cooling below 2 K, a steep increase in the heat capacity of $CaCu_3Ru_4O_{12}$ is observed. Having established accurate values of the electric-field gradients at the Cu and Ru sites by NQR and accounting for the different isotopical abundances, a corresponding nuclear Schottky anomaly has been calculated and subtracted from the raw data of the low-temperature heat capacity of $CaCu_3Ru_4O_{12}$. The result is a logarithmic increase in C/T over an order of magnitude of 2 K down to 200 mK which is a hallmark for non-Fermi-liquid behavior. The specific heat of $CaCu_3Ru_4O_{12}$ below 10 K is shown in Fig. 7. The black squares correspond to the measured raw data and the red circles are corrected for the nuclear Schottky contribution, whereas the red line indicates the logarithmic increase in C/T versus T for decreasing T. However, below 0.1 K, the values of the heat capacity lie above this expected logarithmic increase. On the basis of NQR experiments that show neither a significant line broadening nor a temperature-dependent line shift, we can exclude residual internal fields as the origin of this anomalous increase. Similar unexplained upturns in C/T have been observed in a large number of heavy-fermion compounds including the stoichiometric non-Fermi-liquid $YbRh_2Si_2$ (Ref. 21 and references therein).

For a closer inspection of the NFL behavior in $CaCu_3Ru_4O_{12}$ at temperatures below 2 K, we have per-

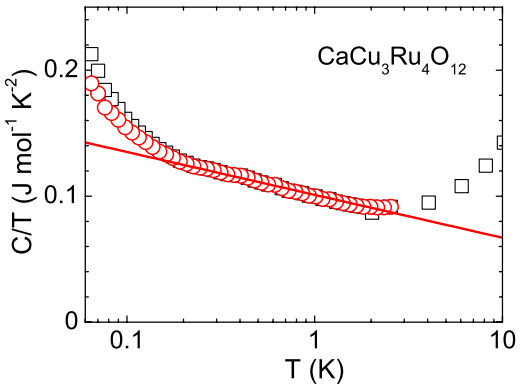

FIG. 7. (Color online) Semilogarithmic representation of the specific heat $C/T(T)$ of polycrystalline $CaCu_3Ru_4O_{12}$ at low temperatures. Black squares correspond to the measured raw data and red circles are corrected for a nuclear Schottky anomaly with values of the electric-field gradients determined by NMR. The full line is a fit according to $C/T=\alpha \ln T+\gamma$ with fitting parameters $\alpha=-16.6$ mJ mol^{-1} K^{-2} and $\gamma=100$ mJ mol^{-1} K^{-2}.

formed ^{63}Cu NQR measurements of the spin-lattice relaxation time T_1. NQR is necessary here because the NMR spectra are strongly broadened by electric-quadrupole effects (see upper frames of Figs. 5 and 6) which prevent a complete excitation of all spectral contributions within one pulse. Hence, the complete information about the spin-lattice relaxation in this system can only be obtained by irradiation of the narrow NQR lines which exhibit a temperature-independent line width [full width at half maximum (FWHM)] $\Delta\nu_{\mathrm{NQR}} \leq 100$ kHz. The values for T_1 are obtained by irradiating the $\pm 1/2 \leftrightarrow \pm 3/2$ NQR transitions of ^{63}Cu (see lower frame of Fig. 5) and fitting the magnetization recovery according to the equation[22]

$$M(t) = 2M_0 \exp\left[-\left(\frac{3t}{T_1}\right)^{\beta}\right], \qquad (1)$$

where the factor 2 arises from the inversion-recovery technique and the exponent β accounts for a stretched exponential behavior of the spin-lattice relaxation.

The upper part of Fig. 8 shows the temperature dependence of the spin-lattice relaxation rate $1/T_1$ of $CaCu_3Ru_4O_{12}$ in a double-logarithmic representation. Red squares refer to the results of the present measurements whereas the blue circles provide a comparison with a previous NQR study[20] for temperatures above 5 K. According to Kato *et al.*,[20] $CaCu_3Ru_4O_{12}$ forms a Fermi-liquid state below $T_F=20$ K, and therefore, should exhibit a Korringa behavior $T_1T=$constant (dashed line in Fig. 8). Such a Korringa behavior was derived from $1/T_1$ in a very restricted temperature range of $5 \leq T \leq 20$ K.[20] The temperature dependence of T_1 according to the Korringa relation $T_1T=$constant is regarded as fingerprint of Fermi liquids in metals and also holds for Fermi liquids in dilute[23] as well as dense Kondo systems.[24] However, the measurements of $1/T_1$ reveal deviations from a Korringa law upon extending the temperature range toward lower temperatures. The data are best described by a power law $1/T_1 \propto T^{0.88}$ within 190 mK$\leq T \leq$14 K

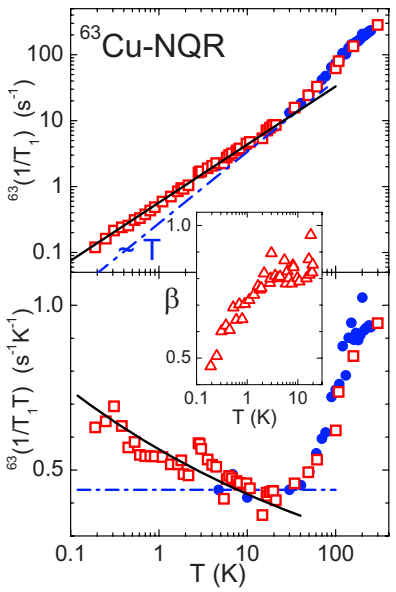

FIG. 8. (Color online) Upper part: temperature dependence of the spin-lattice relaxation rate $1/T_1$ of polycrystalline $CaCu_3Ru_4O_{12}$ in a double-logarithmic representation. The results of the present study (red squares) are in good agreement with the values reported in the literature (blue circles) by Kato *et al.* (Ref. 20) for $T \geq 5$ K. Deviations from a Korringa law $1/T_1 \propto T$ (dashed line) are observed. The solid line shows a fit to a power-law dependence $1/T_1 \propto T^{0.88}$ within 190 mK$\leq T \leq$14 K. Lower part: $1/T_1T$ versus T in a semilogarithmic plot. The Korringa law (Ref. 20) corresponds to a constant value (blue dashed line). A clear increase in cooling is observed—described by $1/T_1T \propto T^{-0.12}$ (black curve). The inset shows the stretching exponent $\beta(T)$ of the magnetization recovery [according to Eq. (1)].

(solid line in Fig. 8). The deviations from a Korringa behavior become much more pronounced when plotting $1/T_1T$ versus T on a linear scale, as shown in the lower part of Fig. 8. A deviation from the Korringa relation $1/T_1 \propto T$ in favor of a power-law dependence, $1/T_1 \propto T^{\alpha}$ with $\alpha<1$, is found to be a characteristic of NFL behavior in a number of compounds.[25–27]

A stretched exponential according to Eq. (1) is necessary to satisfactorily describe the magnetization recovery. The introduction of a stretching exponent β is often used to parametrize a distribution of spin-lattice relaxation rates.[27,28] The temperature dependence of β is shown in the inset of Fig. 8. At elevated temperatures, $T>20$ K, the relaxation is best described by a single exponential magnetization recovery ($\beta=1$, not shown), whereas it exhibits stretched exponential behavior with β decreasing to $\sim$0.5 toward the lowest temperatures. A stretching exponent $\beta=0.5$ is expected in the case of a nuclear spin-lattice relaxation which is governed by independently fluctuating electronic paramagnetic centers.[29]

V. DISCUSSION AND CONCLUSION

The formation of a heavy-fermion state is based on the interaction between localized and itinerant electronic states. The requirement for these two different electronic sub-

systems is obviously fulfilled in traditional *f*-electron (localized) intermetallic (itinerant) heavy-fermion compounds. The situation is much less clear in the few cases of *d*-electron-based heavy fermions. LiV_2O_4 is the first example of a transition-metal oxide showing canonical heavy-fermion behavior.[30] LiV_2O_4 crystallizes in the cubic spinel structure, in which the magnetic vanadium ions form a pyrochlore lattice and are subject to strong geometric frustration. Moreover, the vanadium ions are in a mixed-valent state of $V^{+3.5}$. In order to apply the concept of a Kondo mechanism, a model has been proposed[31] in which, on average, one of the 1.5 *d* electrons per vanadium is rather localized and establishes an $S=1/2$ magnetic moment, whereas the remaining 0.5 *d* electrons form a broad band of conduction electrons. On the other hand, frustration of the vanadium ions can also strongly enhance spin fluctuations and results in similar physical properties.[32] Furthermore, neutron scattering revealed the presence of competing ferromagnetic and antiferromagnetic (AFM) interactions.[33,34] Detailed NMR studies on LiV_2O_4 demonstrated an extreme sensitivity of the physical properties on the magnetic defect concentration.[35,36] The low-temperature specific heat of polycrystalline LiV_2O_4 could be best described by a NFL model in the vicinity of a quantum critical point (QCP), where minor doping of Zn or Ti induces a magnetically ordered state.[37] Despite continuous theoretical efforts, the physical origin of the heavy-fermion behavior of LiV_2O_4 is still under debate.[38,39]

Apart from the exceptional case of LiV_2O_4, heavy-fermion-like and NFL behaviors have been found (in particular) among the ruthenates, notably, $La_4Ru_6O_{19}$,[40] $Sr_3Ru_2O_7$,[41,42] $CaRuO_3$,[43] and $Ca_{2-x}Sr_xRuO_4$.[44] In the case of $La_4Ru_6O_{19}$, the specific heat shows a minimum around 5 K, followed by a strong increase upon further cooling with a characteristic $\ln T$ dependence below 1 K.[40] Furthermore, a linear *T* dependence of the resistivity $\rho(T)$ is observed below 30 K. The temperature dependences of both $C/T(T)$ and $\rho(T)$ of $La_4Ru_6O_{19}$ are likewise found in the prototypical *f*-electron-based NFL system $CeCu_{6-x}Au_x$.[45] The two distinct electronic subsystems in $La_4Ru_6O_{19}$ are both derived from Ru *d* electrons: strong Ru-O orbital hybridization gives rise to broad bands of delocalized states, whereas Ru-Ru bonds form dimerized localized states (narrow bands) near the Fermi energy.[40] In general, the large size of orbitals in itinerant (Ru) 4*d* transition-metal oxides results in wide bands with corresponding large kinetic energy. The subtle balance between the kinetic energy and many-body interactions of other electrons from transition metal-oxygen bonds may give rise to additional localized electronic states that are referred to as a self-organized critical state.[40]

The anomalous strong increase in the specific heat toward lowest temperatures beyond the characteristic $\ln T$ dependence in $CaCu_3Ru_4O_{12}$ is a property likewise observed further in other ruthenates. Metallic $Sr_3Ru_2O_7$ exhibits NFL behavior in the vicinity of a magnetic-field-induced QCP.[41,42] In this case, Mössbauer data provided an upper limit of the electric-field gradient at the Ru site (assumed to hold true also for the Sr site) that allowed one to calculate a corresponding Schottky contribution.[46] However, the experimentally observed increase in the specific heat is much stronger.[46] This situation is also found for Sr_2RuO_4 where a low-temperature upturn of the specific heat can be described by the high-temperature tail of a Schottky anomaly.[47,48] Again, the experimentally determined Schottky contribution is orders of magnitude larger than the calculated quadrupolar contribution.[47,48]

Another aspect concerns the physical classification of $CaCu_3Ru_4O_{12}$. Recent x-ray spectroscopic investigations[7] revealed a direct analogy to conventional *f*-electron-based heavy-fermion systems in the localized magnetic moments originated from Cu^{2+} ions and itinerant conduction electrons from strong orbital Ru-O hybridization. The formation of a heavy-fermion state, as reported recently,[5] is confirmed by the present investigation due to the Fermi-liquid behavior of the electrical resistivity combined with the enhanced Sommerfeld coefficient. On the other hand, the magnetic susceptibility exhibits a typical mixed-valent behavior. In this respect it is interesting to note that the *f*-electron-based compounds $Ce_2T_3X_9$ (T=Rh, Ir and X=Al, Ga) show heavy-fermion behavior in their transport properties but mixed-valence characteristics in their magnetic susceptibility,[49,50] indicative of two different energy scales. Moreover, the Kondo temperature T_K of *f*-electron heavy-fermion compounds exhibiting NFL behavior in the vicinity of an antiferromagnetic quantum critical point can be inferred by extrapolating the logarithmic increase in the low-temperature specific heat toward high temperatures. The temperature, when C/T becomes zero, is identified with T_K. In the present case of $CaCu_3Ru_4O_{12}$, this results in a Kondo temperature of about 440 K compared to 870 K that is estimated above on the basis of the Sommerfeld coefficient. These values are subject to large error bars due to the extended extrapolations involved, but characteristic temperatures T_K and T_{SF} of several hundred degrees (in combination with a moderate Sommerfeld coefficient) are compatible with a mixed-valence scenario and, in particular, reminiscent of $CeRu_2$.

In any case, x-ray spectroscopy suggests a well-defined electronic system in $CaCu_3Ru_4O_{12}$ analogous to traditional *f*-electron-based heavy-fermion systems. In this situation, the experimentally observed NFL behavior may be compared to different theoretical models. These include the multichannel Kondo effect[51] or order-parameter fluctuations of a second-order quantum phase transition at $T=0$ K.[52,53] Since most NFL compounds occur in substitutional series with inherent disorder, alternative specific models relating NFL properties primarily to disorder have been developed—in particular based on a statistical distribution of Kondo temperatures[54] or in terms of Griffiths singularities.[55] For a three-dimensional (3D) antiferromagnetic quantum phase transition,[52] a $\ln T$ dependence of the specific heat is expected, whereas a disorder-driven cluster formation within a paramagnetic matrix (Griffiths phase)[55] predicts a temperature dependence of the specific heat according to $C(T)/T \propto T^{-1+\lambda}$ with $\lambda=1$ for a Fermi liquid and $\lambda<1$ in the NFL regime.

In Fig. 9 the low-temperature specific-heat data of $CaCu_3Ru_4O_{12}$ are shown in a double-logarithmic presentation and fitted either by $C(T)=\alpha T \ln(T)+\gamma T$ (AFM quantum phase transition[52]) or by $C(T)=cT^{\lambda}$ according to the disorder NFL model.[55] Evidently, there are only slight differences between these two models, and the experimental data can be satisfactorily described by either of them. The disorder

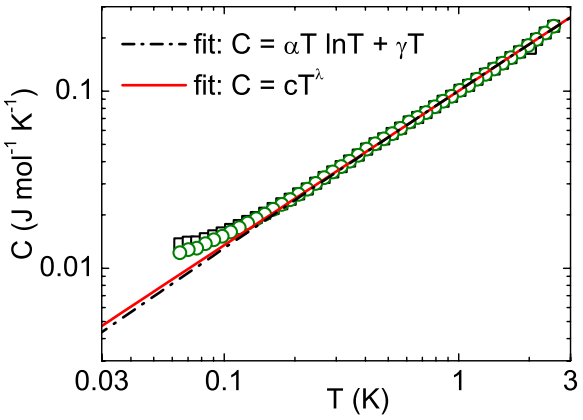

FIG. 9. (Color online) Specific heat $C/T(T)$ of polycrystalline $CaCu_3Ru_4O_{12}$ in a double-logarithmic representation. The black squares correspond to the measured raw data and the green circles are corrected for a nuclear Schottky anomaly as described in the text. Two different fits according to an AFM quantum phase transition and a disorder-driven NFL state are indicated by the black and red lines, respectively.

model yields a fitting constant of $\lambda = 0.87$ which is exactly in the range of values found in a number of uranium-based NFL heavy fermions.[56] It is interesting to note that the concept of Griffiths singularities has been resumed in order to classify quantum phase transitions in itinerant magnets.[57] There, the inherent quantum dynamics were supposed to manifest in a broad distribution of magnetic relaxation rates, which we observed in a stretched exponential magnetization recovery according to Eq. (1) in NQR experiments.

In summary, we have investigated $CaRu_3Ru_4O_{12}$ by bulk magnetic, thermodynamic, transport, and NMR measurements. The results consistently describe $CaCu_3Ru_4O_{12}$ as a correlated metal with a high spin-fluctuation temperature and NFL behavior below 2 K. Until now, $CaCu_3Ru_4O_{12}$ seems to be the best analog of a transition-metal oxide to traditional *f*-electron-based heavy-fermion compounds exhibiting NFL behavior in the vicinity of a quantum critical point.

ACKNOWLEDGMENTS

This work was supported by the Deutsche Forschungsgemeinschaft (DFG) via research unit 960 "Quantum Phase Transitions," Sonderforschungsbereich 484 (Augsburg), DFG (Contract No. SCHE487/7) and by the project COST P16 ECOM of the European Union.

*alexander.krimmel@physik.uni-augsburg.de

[1] C. C. Homes, T. Vogt, S. M. Shapiro, S. Wakimoto, and A. P. Ramirez, Science **293**, 673 (2001).
[2] P. Lunkenheimer, R. Fichtl, S. G. Ebbinghaus, and A. Loidl, Phys. Rev. B **70**, 172102 (2004), and references therein.
[3] Z. Zeng, M. Greenblatt, M. A. Subramanian, and M. Croft, Phys. Rev. Lett. **82**, 3164 (1999).
[4] R. Weht and W. E. Pickett, Phys. Rev. B **65**, 014415 (2001).
[5] W. Kobayashi, I. Terasaki, J. Takeya, I. Tsukada, and Y. Ando, J. Phys. Soc. Jpn. **73**, 2373 (2004).
[6] H.-A. Krug von Nidda, R. Bulla, N. Büttgen, M. Heinrich, and A. Loidl, Eur. Phys. J. B **34**, 399 (2003).
[7] T. T. Tran, K. Takubo, T. Mizokawa, W. Kobayashi, and I. Terasaki, Phys. Rev. B **73**, 193105 (2006).
[8] J. Rodriguez-Carvajal, Physica B **192**, 55 (1993).
[9] R. Bachmann, F. J. DiSalvo, Jr., T. H. Geballe, R. L. Greene, R. E. Howard, C. N. King, H. C. Kirsch, K. N. Lee, R. E. Schwall, H.-U. Thomas, and R. E. Zubeck, Rev. Sci. Instrum. **43**, 205 (1972).
[10] S. G. Ebbinghaus, A. Weidenkaff, and R. J. Cava, J. Solid State Chem. **167**, 126 (2002).
[11] M. Labeau, B. Bochu, J. C. Joubert, and J. Chenavas, J. Solid State Chem. **33**, 257 (1980).
[12] R. H. Blessing, Acta Crystallogr., Sect. A: Found. Crystallogr. **51**, 33 (1995).
[13] G. M. Sheldrick, Acta Crystallogr., Sect. A: Found. Crystallogr. **64**, 112 (2008).
[14] M. A. Subramanian and A. W. Sleight, Solid State Sci. **4**, 347 (2002).
[15] J. Lawrence, Phys. Rev. B **20**, 3770 (1979).
[16] A. V. Tsvyashchenko, L. N. Fomicheva, A. A. Sorokin, G. K. Ryasny, B. A. Komissarova, L. G. Shpinkova, K. V. Klementiev, A. V. Kuznetsov, A. P. Menushenkov, V. N. Trofimov, A. E. Primenko, and R. Cortes, Phys. Rev. B **65**, 174513 (2002).
[17] Y. Kishimoto, Y. Kawasaki, and T. Ohno, Phys. Lett. A **317**, 308 (2003).
[18] A. C. Hewson and J. W. Rasul, J. Phys. C **16**, 6799 (1983).
[19] H. Kato, T. Tsuruta, T. Nishioka, M. Matsumura, H. Sakai, and S. Kambe, J. Magn. Magn. Mater. **310**, e51 (2007).
[20] H. Kato, T. Tsuruta, T. Nishioka, M. Matsumura, H. Sakai, and S. Kambe, J. Phys. Chem. Solids **68**, 2187 (2007).
[21] O. Trovarelli, C. Geibel, S. Mederle, C. Langhammer, F. M. Grosche, P. Gegenwart, M. Lang, G. Sparn, and F. Steglich, Phys. Rev. Lett. **85**, 626 (2000).
[22] J. Chepin and J. H. Ross, J. Phys.: Condens. Matter **3**, 8103 (1991).
[23] H. Shiba, Prog. Theor. Phys. **54**, 967 (1975).
[24] Y. Kitaoka, S. Kawasaki, T. Mito, and Y. Kawasaki, J. Phys. Soc. Jpn. **74**, 186 (2005).
[25] T. Omuta, K. Fujiwara, J. Takeuchi, Y. Kohori, and T. Kohara, Physica B **259-261**, 378 (1999).
[26] R. E. Walstedt, H. Kojima, N. Butch, and N. Bernhoeft, Phys. Rev. Lett. **90**, 067601 (2003).
[27] B.-L. Young, D. E. MacLaughlin, M. S. Rose, K. Ishida, O. O. Bernal, H. G. Lukefahr, K. Heuser, and G. R. Stewart, Phys. Rev. B **70**, 174430 (2004).
[28] D. C. Johnston, Phys. Rev. B **74**, 184430 (2006).
[29] D. Tse and S. R. Hartmann, Phys. Rev. Lett. **21**, 511 (1968).
[30] S. Kondo, D. C. Johnston, C. A. Swenson, F. Borsa, A. V. Mahajan, L. L. Miller, T. Gu, A. I. Goldman, M. B. Maple, D. A. Gajewski, E. J. Freeman, N. R. Dilley, R. P. Dickey, J. Merrin, K. Kojima, G. M. Luke, Y. J. Uemura, O. Chmaissem, and J. D.

Jorgensen, Phys. Rev. Lett. **78**, 3729 (1997).
[31] V. I. Anisimov, M. A. Korotin, M. Zölfl, T. Pruschke, K. Le Hur, and T. M. Rice, Phys. Rev. Lett. **83**, 364 (1999).
[32] C. Urano, M. Nohara, S. Kondo, F. Sakai, H. Takagi, T. Shiraki, and T. Okubo, Phys. Rev. Lett. **85**, 1052 (2000).
[33] A. Krimmel, A. Loidl, M. Klemm, S. Horn, and H. Schober, Phys. Rev. Lett. **82**, 2919 (1999).
[34] A. P. Murani, A. Krimmel, J. R. Stewart, M. Smith, P. Strobel, A. Loidl, and A. Ibarra-Palos, J. Phys.: Condens. Matter **16**, S607 (2004).
[35] H. Kaps, M. Brando, W. Trinkl, N. Büttgen, A. Loidl, E.-W. Scheidt, M. Klemm, and S. Horn, J. Phys.: Condens. Matter **13**, 8497 (2001).
[36] X. Zong, S. Das, F. Borsa, M. D. Vannette, R. Prozorov, J. Schmalian, and D. C. Johnston, Phys. Rev. B **77**, 144419 (2008).
[37] M. Brando, N. Büttgen, V. Fritsch, J. Hemberger, H. Kaps, H.-A. Krug von Nidda, M. Nicklas, K. Pucher, W. Trinkl, A. Loidl, E.-W. Scheidt, M. Klemm, and S. Horn, Eur. Phys. J. B **25**, 289 (2002).
[38] R. Arita, K. Held, A. V. Lukoyanov, and V. I. Anisimov, Phys. Rev. Lett. **98**, 166402 (2007).
[39] V. Yushankhai, A. Yaresko, P. Fulde, and P. Thalmeier, Phys. Rev. B **76**, 085111 (2007).
[40] P. Khalifah, R. Jin, Y. Liu, A. P. Ramirez, and R. J. Cava, Nature (London) **411**, 669 (2001).
[41] S. A. Grigera, R. S. Perry, A. J. Schofield, M. Chiao, S. R. Julian, G. G. Lonzarich, S. I. Ikeda, Y. Maeno, A. J. Millis, and A. P. Mackenzie, Science **294**, 329 (2001).
[42] R. S. Perry, L. M. Galvin, S. A. Grigera, L. Capogna, A. J. Schofield, A. P. Mackenzie, M. Chiao, S. R. Julian, S. Ikeda, S. Nakatsuji, Y. Maeno, and C. Pfleiderer, Phys. Rev. Lett. **86**, 2661 (2001).
[43] L. Klein, L. Antognazza, T. H. Geballe, M. R. Beasley, and A. Kapitulnik, Physica B **259-261**, 431 (1999).
[44] S. Nakatsuji, D. Hall, L. Balicas, Z. Fisk, K. Sugahara, M. Yoshioka, and Y. Maeno, Phys. Rev. Lett. **90**, 137202 (2003).
[45] H. von Löhneysen, J. Phys.: Condens. Matter **8**, 9689 (1996).
[46] Z. X. Zhou, S. McCall, C. S. Alexander, J. E. Crow, P. Schlottmann, A. Bianchi, C. Capan, R. Movshovich, K. H. Kim, M. Jaime, N. Harrison, M. K. Haas, R. J. Cava, and G. Cao, Phys. Rev. B **69**, 140409(R) (2004).
[47] C. Langhammer, F. Steglich, M. Lang, and T. Saski, Eur. Phys. J. B **26**, 413 (2002).
[48] K. Pucher, J. Hemberger, F. Mayr, V. Fritsch, A. Loidl, E.-W. Scheidt, S. Klimm, R. Horny, S. Horn, S. G. Ebbinghaus, A. Reller, and R. J. Cava, Phys. Rev. B **65**, 104523 (2002).
[49] B. Buschinger, C. Geibel, M. Weiden, C. Dietrich, G. Cordier, G. Olesch, J. Köhler, and F. Steglich, J. Alloys Compd. **260**, 44 (1997).
[50] B. Buschinger, O. Trovarelli, M. Weiden, C. Geibel, and F. Steglich, J. Alloys Compd. **275-277**, 633 (1998).
[51] P. Schlottmann and P. D. Sacramento, Adv. Phys. **42**, 641 (1993).
[52] A. J. Millis, Phys. Rev. B **48**, 7183 (1993).
[53] S. Sachdev, N. Read, and R. Oppermann, Phys. Rev. B **52**, 10286 (1995).
[54] O. O. Bernal, D. E. MacLaughlin, H. G. Lukefahr, and B. Andraka, Phys. Rev. Lett. **75**, 2023 (1995).
[55] A. H. Castro Neto, G. Castilla, and B. A. Jones, Phys. Rev. Lett. **81**, 3531 (1998).
[56] M. C. de Andrade, R. Chau, R. P. Dickey, N. R. Dilley, E. J. Freeman, D. A. Gajewski, M. B. Maple, R. Movshovich, A. H. Castro Neto, G. Castilla, and B. A. Jones, Phys. Rev. Lett. **81**, 5620 (1998).
[57] T. Vojta and J. Schmalian, Phys. Rev. B **72**, 045438 (2005).